

## Molded Neoprene Liner Pads for the Poseidon Missile Launcher

J. F. MEIER, H. F. MINTER, and H. J. CONNORS,  
*Westinghouse Research Laboratories, Pittsburgh, Pennsylvania 15235*

### Synopsis

Neoprene formulations and mechanical designs have been developed to meet special operational requirements for the Poseidon Missile Launch System liner. The liner supports the missile in an aligned position, provides shock mitigation, reacts properly with the missile during launch, and damps vibrations. Operational requirements include static and dynamic compressive stiffness, damping, and water drainability. A mechanical design was evolved that utilized notched, prebuckled struts as supporting members. Compression-deflection characteristics were modified by simultaneous changes in geometrical design and polymer formulation. A study of the effects of variations in polymer compounding and mechanical design on the compressive stiffness, rate sensitivity of the compression-deflection characteristics, and vibrational damping is described. Mold release agents and their role in successful production are discussed.

### INTRODUCTION

In the early 1960s, the U.S. Navy decided to modify some missile-carrying nuclear submarines from Polaris-type missiles to the considerably larger Poseidon missile. To accommodate the greater diameter of the Poseidon missile a conceptual change of design and materials was required. As described in this paper, a transfer-molded neoprene launch tube liner material was developed for use in the Poseidon Missile Launch System. Liner pads, each weighing ~5.6 lb, are attached with adhesive to the launch tube to provide an interface between the missile and the launch tube (Fig. 1). The liner must support the missile in the launch tube in an aligned position, provide shock mitigation, exhibit vibration transmissibility properties compatible with missile response characteristics, and react properly with the missile during eject from the launcher.

Liner pads are reuseable, readily drainable, have adequate mechanical strength to withstand the forces developed during launch, are flame resistant, and will not degrade on extended exposure to sea water.

A critical relationship between polymer formulation and mechanical configuration was found necessary to meet the operational requirements of static compressive stiffness, shear stiffness, damping, and durability.

A compatible mechanical design and neoprene formulation were developed that gave satisfactory results on flat, small-scale laboratory sam-

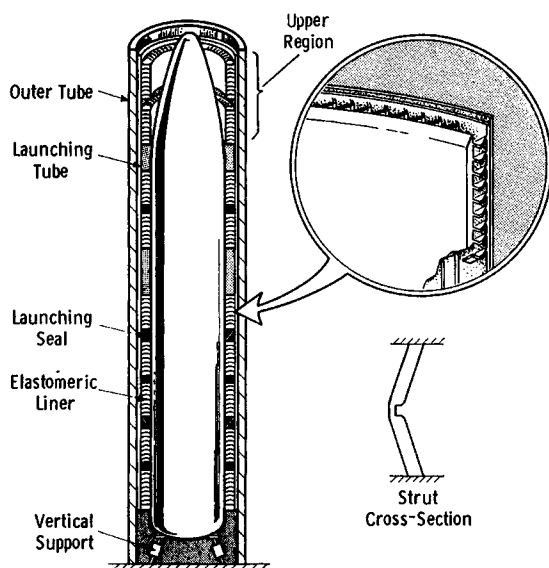


Fig. 1. Schematic launcher tube.

ples. Full-scale, curved, strutted modules were molded on a pilot basis preliminary to the present fabrication in production.

Development of the mechanical design and the selection of polymer for full-scale modules is discussed and typical test results are presented. It was imperative that compound development and mechanical testing be simultaneously integrated. However, for the sake of clarity, this paper will treat three separate sections: (1) testing, (2) compound development, and (3) developmental molding and production.

## TESTING

In order to support the missile in the proper manner and to ensure its integrity, the elastomeric shock absorber must possess certain functional characteristics.

### Compression-Deflection Characteristics

Figure 2 shows the maximum allowable dynamic load-deflection curve at a  $2500 \text{ min}^{-1}$  strain rate and the maximum and minimum static load-deflection curves for a  $1 \text{ min}^{-1}$  strain rate. The limits are for first cycles on conditioned samples. (A conditioned sample is one that has been statically compressed 60% after production and allowed to recover for a minimum of 24 hr before testing.)

In the static load-deflection test, the sample is consecutively deflected four times to 60% of the original height without pause. As shown in Figure 3, the pseudo set, maximum allowable 8%, is the spread between the start of the first-cycle and fourth-cycle loading strokes. In addition, it is

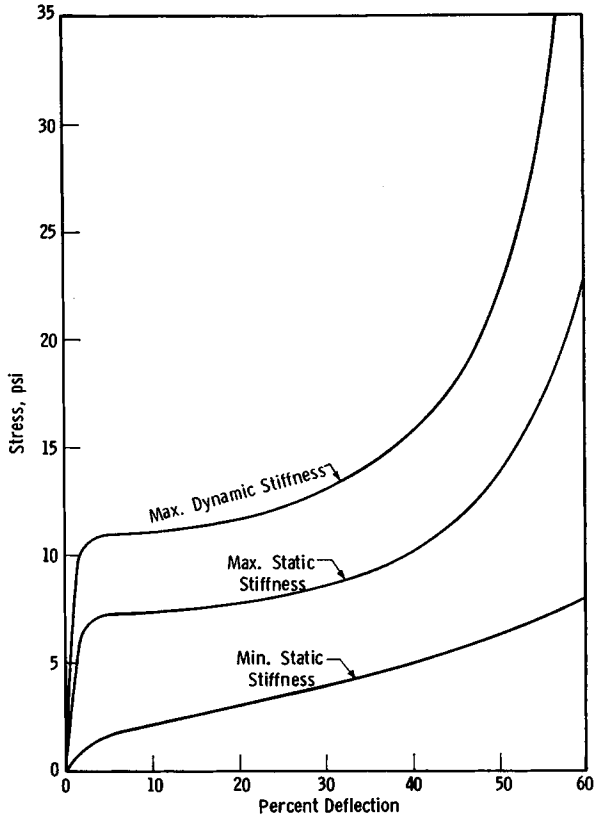


Fig. 2. Compression-deflection (C-D) limits for Poseidon liner material.

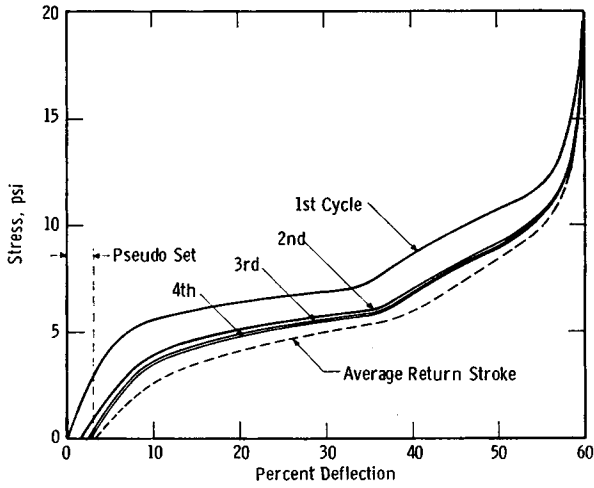


Fig. 3. Four-cycle static compression-deflection curves for an elastomeric liner material.

required that after 1 hr recovery from the initial load-deflection cycle a repeat test be run and that the first cycle of the repeat run must coincide within 15% of the original first-cycle test.

Dynamic load-deflection properties are determined using the drop table schematically shown in Figure 4. A weight guided by a ball bushing bears

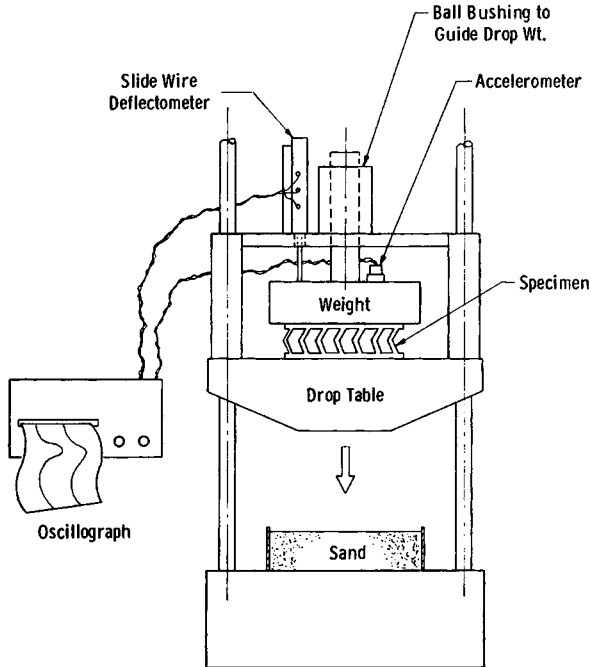


Fig. 4. Drop test for obtaining dynamic compression-deflection data.

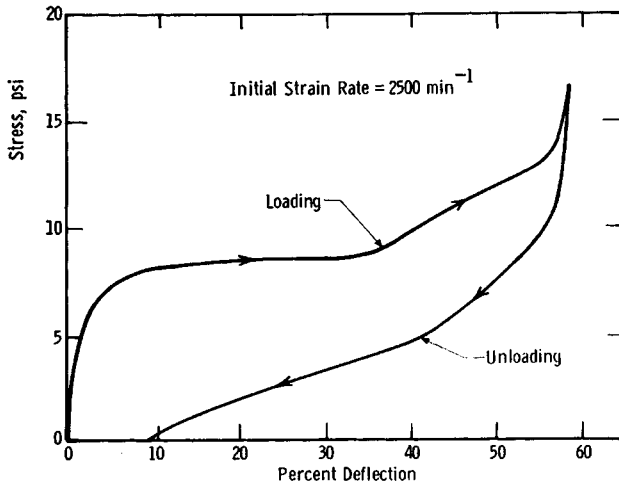


Fig. 5. Dynamic loop for elastomeric structure.

against the test specimen. A deflectometer connected to the weight permits linear deflection under shock to be determined, and an accelerometer mounted on the weight permits the dynamic compressive stress to be determined. Deflection and acceleration traces are recorded on an oscillograph. Figure 5 shows a typical dynamic loop obtained for an elastomeric structure.

### Damping Characteristics

The quality factor,  $Q$ , was specified as 5 or less for a sample precompressed 0.150 in. and cycled  $\pm 0.020$  in. at 10 cps;  $Q = 1/(2C/C_e)$ , where  $C/C_e$  is the damping ratio.

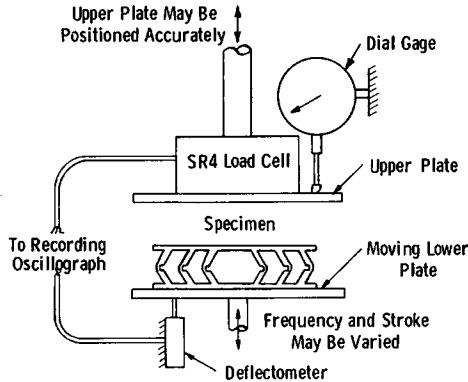


Fig. 6. Test arrangement for measuring damping.

Damping was determined by using the apparatus shown in Figure 6. It consists of a lower plate that vibrates sinusoidally and whose amplitude and frequency can be varied, and an upper plate that can be positioned to regulate the precompression of the structure. A load cell mounted on the upper plate permits the specimen stress to be monitored, and a deflectometer is attached to the moving plate. Stresses and deflections are recorded on an oscillograph as a hysteresis loop. Figure 7 shows a typical loop and the method used for calculating the  $Q$  value.

### Shear Tests

In order to insure slippage between the liner and the missile to prevent "wind up" of the liner during missile loading and alignment, the liner must evidence a minimum of 2.5 psi at 10% shear strain. Sufficient shear stiffness also insures that the proper mode of compressive buckling is obtained for an annular configuration in which the liner experiences both shear and compressive loads. The shear properties are determined in the manner shown in Figure 8. Shear strain is applied at a rate of approximately  $1 \text{ min.}^{-1}$ . The shear properties are obtained with the struts oriented as shown and also with the struts rotated 90 degrees.

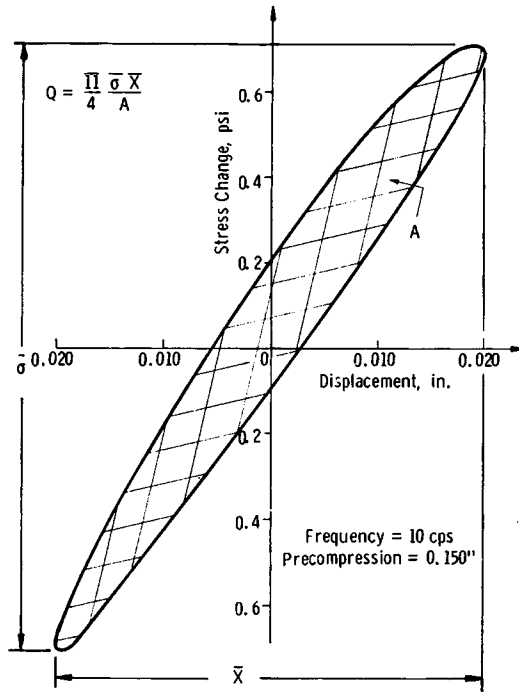


Fig. 7. Typical hysteresis loop for determining damping.

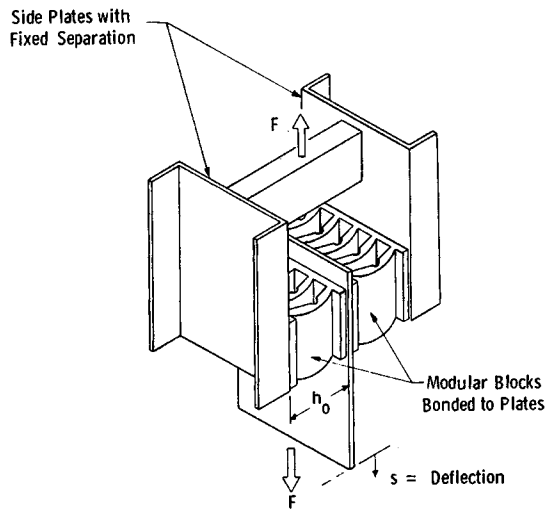


Fig. 8. Shear test arrangement (axial direction).

### Mechanical Design of Elastomeric Structures

Structures composed of two flat surfaces joined by straight columns were initially considered (Fig. 9) but were soon rejected as the early portion of both the static and dynamic load deflection curves (Fig. 10) exhibits a spike.

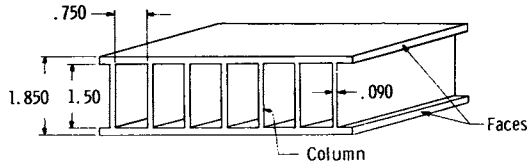


Fig. 9. Box structure with uniform columns.

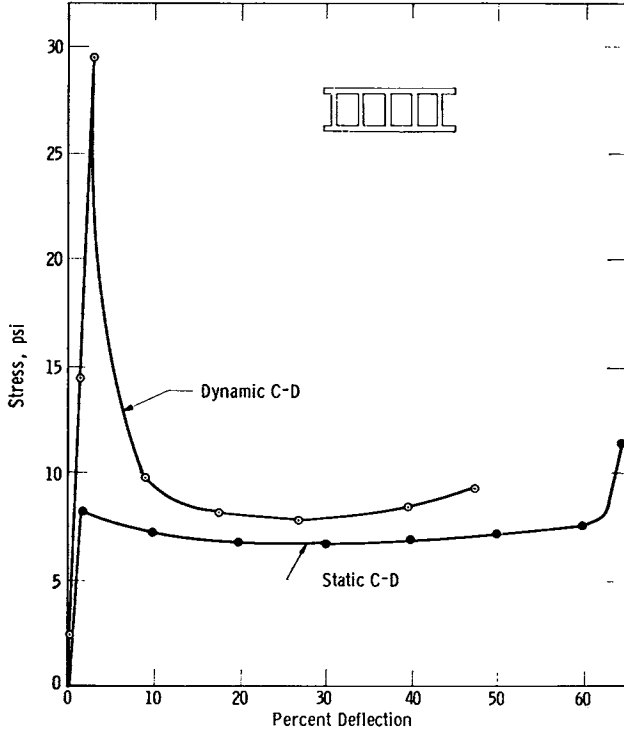


Fig. 10. Compression-deflection curves for box structure of Figure 9.

The spike at low deflections is understandable when it is observed that as the static buckling load is approached, the column develops a considerable bow. If, under dynamic loading, the strut does not have time to “fly out,” a large compressive load can develop before strut buckling occurs. As shown in Figure 11, prebuckling the column structure reduces the sharp dynamic spike.

Although prebuckling a column reduces the dynamic spike, the general shape of the load-deflection curves for a uniform column is undesirable.

The shape of the load-deflection curve requires careful attention to design in order to achieve the steep initial rise, the plateau which follows it, and a controlled stiffness to bottoming. In order to modify the shape of the load-deflection curves, several strut modifications were considered and eval-

uated. A notched strut gave promising results, and Figure 12 shows the basic difference in compressed shape for a strut of uniform thickness and a notched strut. The notch was found to lower the front end and raise the rear end of the load deflection curve, thereby eliminating the undesirable characteristics exhibited by a uniform column.

Initially, notched and prebuckled struts were made in two steps. A box structure, such as shown in Figure 13a, was cast from polyurethane (Adiprene-MOCA) using mold inserts consisting of standard bar stock to which rectangular metal strips were fastened to form the notches. The box structure was only partially cured (still "green"), the core bars removed, the box prebuckled a specified amount, and the sample fully cured in the buckled

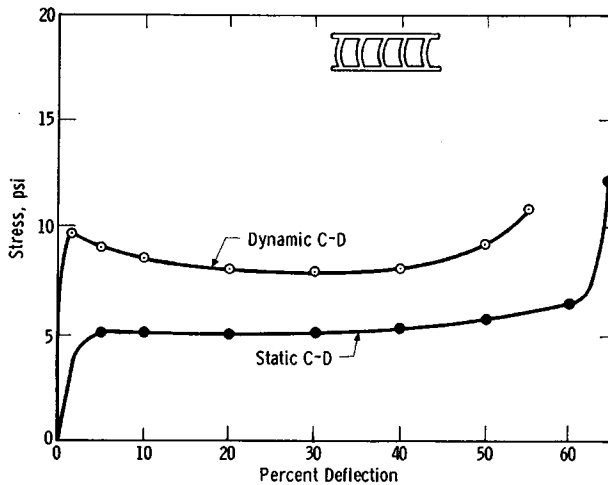


Fig. 11. Effect of prebuckle on compression-deflection curves for box structure of Figure 9.

condition. Figure 13b shows the resulting structure. Later, epoxy bars were cast in the prebuckled urethane structures thereby providing mold inserts with which prebuckled, notched structures could be cast from urethanes of different formulation and with which rubber could be molded. After experience was gained in molding and design, metal inserts having desired contours were machined from steel and aluminum.

Figure 14 shows compression-deflection results for a notched and prebuckled urethane casting that conform much more closely to the desired target than those obtained for a uniform column. Further modifications in the load-deflection characteristics were made by varying the degree of prebuckle, the strut thickness, notch dimensions, and elastomer formulation.<sup>1,2</sup>

A large number of configurations other than buckled, notched structures were evaluated, and the results are published elsewhere.<sup>2</sup>



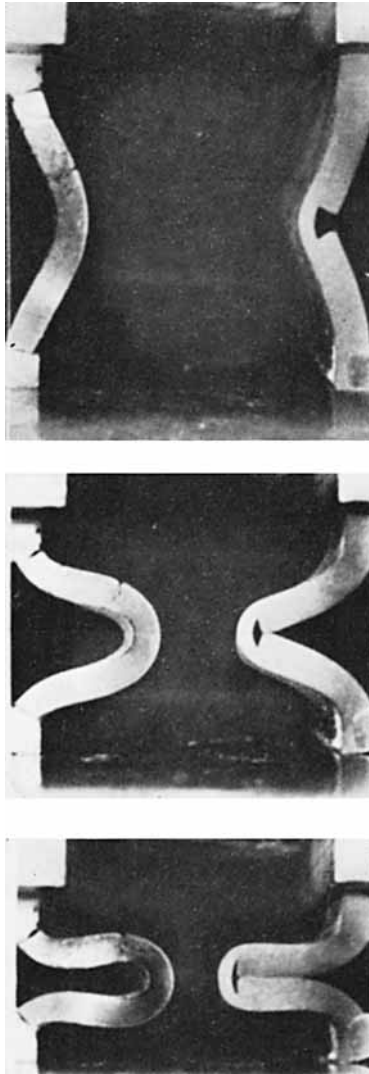


Fig. 12. Comparison of buckling shapes for a uniform column and a notched column.

## COMPOUND DEVELOPMENT

### Polymer Compounding, Molding, and Evaluation

An analysis of the specifications<sup>3</sup> that a candidate material must meet led to the selection of neoprene as a most promising elastomer, mainly because of its flame resistance and ease of adhesive bonding. (Cast polyurethane is also being used for production pads.<sup>2</sup>) Other elastomers such as EPDM and NBR were considered but rejected because of possible bonding problems (Teflon to rubber and rubber to launch tube) or because the dynamic/static (D/S) ratio in initial test formulations exceeded specification

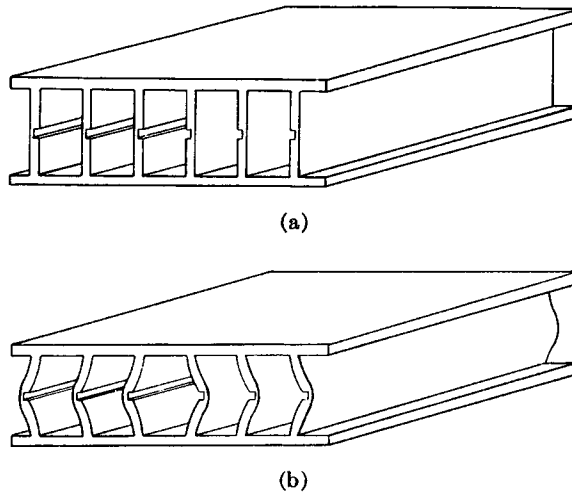


Fig. 13. Two step process for producing notched and prebuckle columns. (a) Simple box is cast, removed "green" from mold before curing, precompressed between plates, and cured. (b) Final prebuckled and notched column.

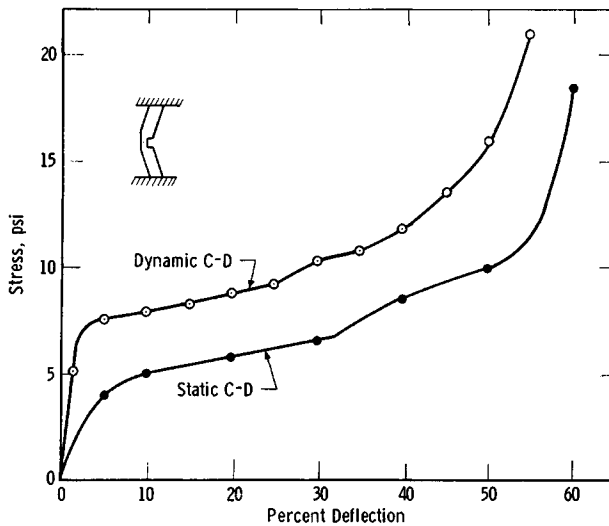


Fig. 14. Typical compression-deflection curves for prebuckled and notched urethane structure.

limits. Compounds of chlorobutyl, neoprene/SBR blends, neoprene/Natsyn 400 blends, neoprene/Budene 501 blends, and Natsyn 400/Budene 501 blends were cursorily examined but rejected because of high D/S ratio or failure to meet the static and dynamic requirements. The main reason for their rejection, however, was the early overall success of neoprene compounding.

### Laboratory Evaluation

On the laboratory scale, each formulation was evaluated by compression molding and testing of strutted modules weighing about 1 lb. In order to evaluate the response of specific compounds, several preparations of each formulation were mill mixed and molded using a uniform strut design and strut thickness. From the static compression-deflection response, changes were made in strut design and thickness and in formulation to adjust the curve to fit the desired static envelope. As experience was gained, formulation G (also coded 808-78, see Table I) and a strut design designated HC-9 (Fig. 15) were used successfully to meet compression-deflection requirements, D/S ratio, and  $Q$  value.<sup>1,4,5</sup> In addition, laboratory modules survived up to 1000 consecutive static cycles to 60% deflection without notch cracking or failure in the strut. Figure 16 shows the typical static compression-deflection response after 100 static cycles to 60% deflection.

An exploded view of the laboratory mold is shown in Figure 17. Opposite ends of alternate bars were provided with spacers to give the desired strut thickness. Core bars were placed in the 6 × 6 in. mold on 0.250 in. thick × ~6 × 1/2 in. metal spacers resting on the bottom plate of the mold and wedged in tightly; two metal spacers ~6 × 1/2 in. × 0.100 in. thick were placed on top of the core bars to fix the face thickness, and the mold was preheated to 300°F. Approximately 480 g rubber was placed on top of the core bars, a preheated 6 × 6 in. × 2 in. thick metal plunger was put in place,

TABLE I  
Physical Properties of Neoprene Compounds

	JM-G or 808-78	HM-24	808-79
WRT Neoprene	100	100	100
Maglite D	4	4	5.3
Neozone A	2	3	2.8
Wingstay 100	—	2	2
Stearic acid	0.5	0.5	0.5
Sundex 790	3	3	2.6
SRF	50	—	—
FT	50	140	140
ZnO	5	5	5.3
Rubberol	—	2.5	2.6
Thionex	1	0.5	0.66
DOTG	1	0.5	1.5
Sulfur	1	0.5	1.0
Tensile strength, psi <sup>a</sup>	2550	1685	1800
Elongation, % <sup>b</sup>	195	195	185
Tensile set, % <sup>c</sup>	1.6	2.8	—
Hardness, Shore A <sup>d</sup>	82	83	81-86

<sup>a</sup> ASTM D-412.

<sup>b</sup> ASTM D-412.

<sup>c</sup> ASTM D-412.

<sup>d</sup> ASTM D-2240.

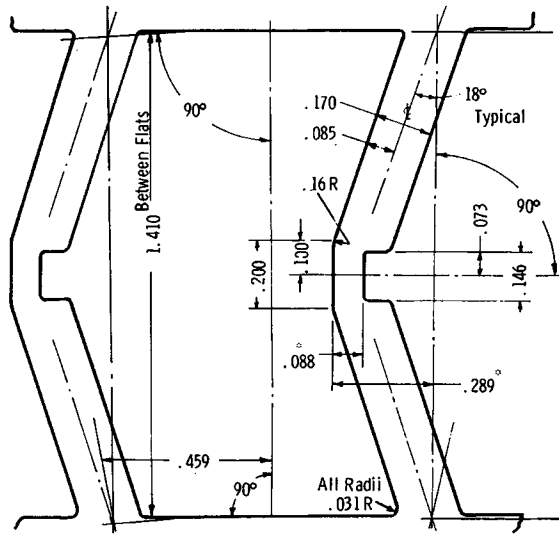


Fig. 15. Strut design HC-9.

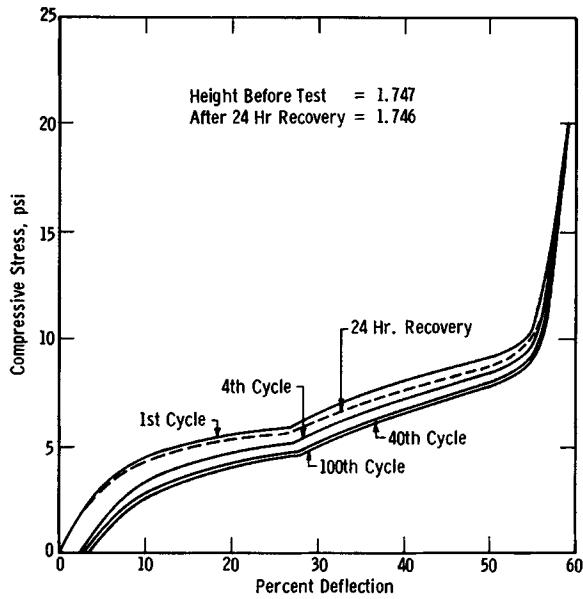


Fig. 16. Static compression-deflection curve for compound JM-G and strut design HC-9 after compression cycling to 60%.

and pressure was applied to transfer the stock between and under the mold inserts. In-mold cure was effected for variable periods of time at 300°F. A 2-hr postcure of the demolded specimen at 300°F was routinely given to ensure an adequate level of cure and to narrow the variance between molded specimens.

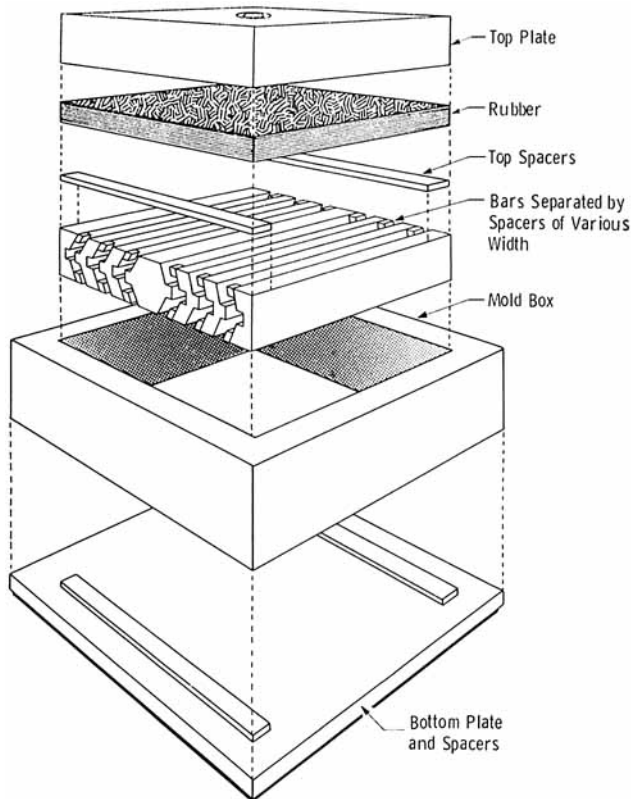


Fig. 17. Exploded view of laboratory mold.

The effect of postcure time at 300°F on molded neoprene pads was studied by determination of crosslink density values. Data shown in Table II were determined using the equilibrium compressive modulus of toluene-swollen pellets as described by Cluff and Gladding.<sup>6</sup> In general, a postcure period tightens the network, thereby effectively reducing processing and molding variations, and imparts stability in physical properties such as compression-deflection response.

The effect of ambient temperature variation on static compressive stiffness response for neoprene pads is shown in Figure 18. Similar data for selected polyurethane formulations are also included.<sup>2,7,8</sup>

Humidity was found to have little or no effect on the neoprene formulation within the time scale of the accelerated experiments.<sup>9</sup>

Carbon black type and loading was found to play a critical role in placement of the compression-deflection curve with respect to stress values.<sup>9</sup> In general, higher black loading or increased black structure (e.g., from FT or MT to HAF) raised stress values. However, stress cracking of the struts on static cycling necessitated tradeoffs between compound stiffness, black loading, and mechanical design.

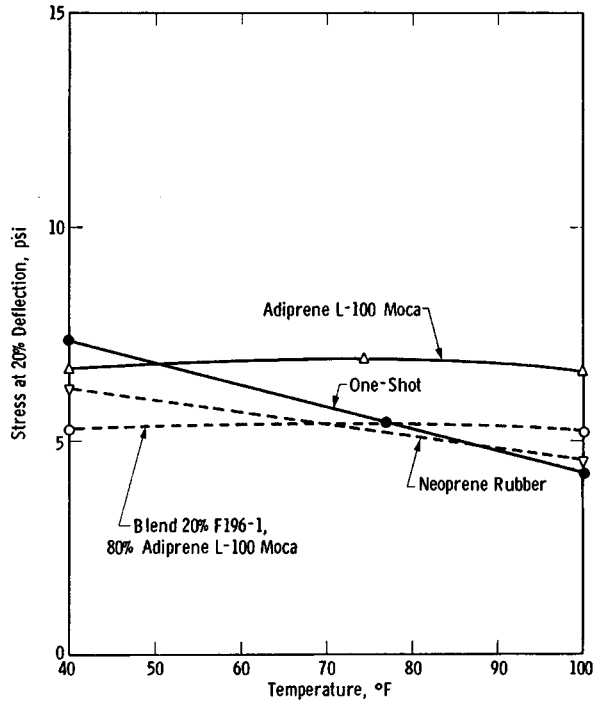


Fig. 18. Static compressive stiffness at 20% deflection vs. temperature.

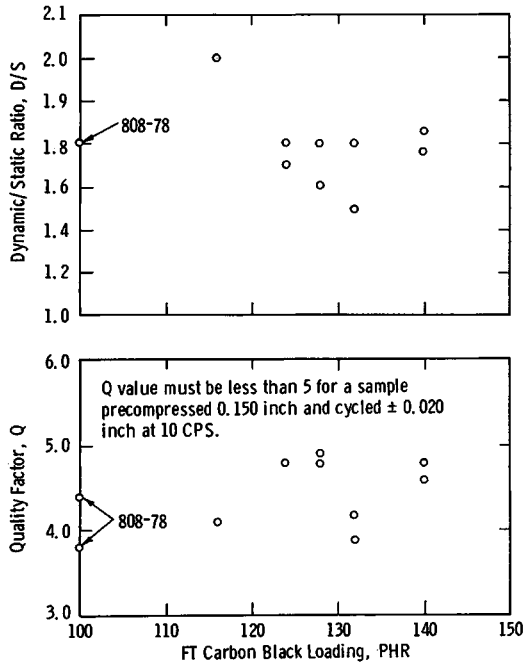


Fig. 19. D/S and Q as a function of FT loading for compound 808-79.

TABLE II  
Crosslink Density Values<sup>a</sup> and  $\bar{M}_c$  of Compounds JM-G and HM-24 as a Function of Postcure Time at 300°F

Postcure Time, at 300°F	Crosslink density, $\nu_e/V$ mole/cc $\times 10^4$		$\bar{M}_c$ , g/mole	
	JM-G	HM-24	JM-G	HM-24
0 (control)	4.28	4.91	3600	3140
1	5.38	—	2860	—
2	—	—	—	—
3	6.63	6.72	2320	2290
5	6.97	7.30	2200	2100
7	6.19	—	2490	—
9	7.43	—	2070	—
10	—	8.00	—	1920

Sp. gr. 1.54 g/cc

$$\frac{\nu_e}{v} = \frac{h_0 S}{3A_0 R T}$$

$h_0$  = height of specimen in cm  
 $S$  = slope of force vs. deflection curve  
 $A_0$  = area of specimen in cm<sup>2</sup>  
 $R$  = gas constant,  $8.21 \times 10^4$  cm g/°K mole  
 $T$  = temperature, °K

$$\bar{M}_c = \frac{d}{\nu_e/v}$$

$\bar{M}_c$  = molecular weight between crosslinks  
 $d$  = density

<sup>a</sup> As determined by Cluff and co-workers.<sup>6</sup>

The D/S ratio and  $Q$  value for a given neoprene type seem fairly well fixed regardless of carbon black loading or compound variation. For example, a compound of neoprene WRT possesses a D/S ratio of  $\sim 1.7$ – $2.0$ <sup>10,11</sup> while a similarly loaded neoprene GRT had D/S value of  $\sim 1.4$ – $1.6$ .<sup>12</sup> Figure 19 shows some values for the D/S ratio as a function of FT loading between 116 and 140 phr for a neoprene WRT compound. The  $Q$  values for the same formulation vary approximately between 4 and 5. D/S and  $Q$  values of compound 808-78 (50 phr FT and 50 phr SRF) are shown for comparison.

The effect of small amounts of polymeric additives on the D/S ratio is rather striking. Incorporation of 4, 8, 12, or 16 parts of nitrile rubber (Paracril BJLT) in a fully compounded WRT formulation with 140 parts FT causes the D/S ratio to increase from the base value of  $\sim 1.7$ – $2.0$  of the WRT-only formulation to 2.16, 2.23, 2.5, and 2.62, respectively, for the nitrile-containing formulations. The  $Q$  values were not determined for these specific formulations. In addition, incorporation of nitrile rubber raises the static stress level above that of the base neoprene formulation. The same sample configuration was used throughout, thereby eliminating shape factor from consideration.

## DEVELOPMENTAL MOLDING AND PRODUCTION

The large development mold is a single-cavity transfer mold consisting of a bottom plate with a concave downward cavity in which the core bars are

placed, a transfer pot with  $\sim 108$  sprue holes of  $\sim 0.090$ -in. diameter, and a plunger or top plate.

The pad surface normally in contact with the missile during stowage and launching must have a low coefficient of friction which is imparted by a Teflon film. A vulcanized composite of sodium-etched Teflon and neoprene is placed in the mold and over the chaplet pins so that the Teflon is concave downward. The core bar assembly is then placed in position. The transfer pot with its numerous sprue holes is placed over the bars, preweighed rubber sheets are added to the transfer pot, and the ram is set in place.

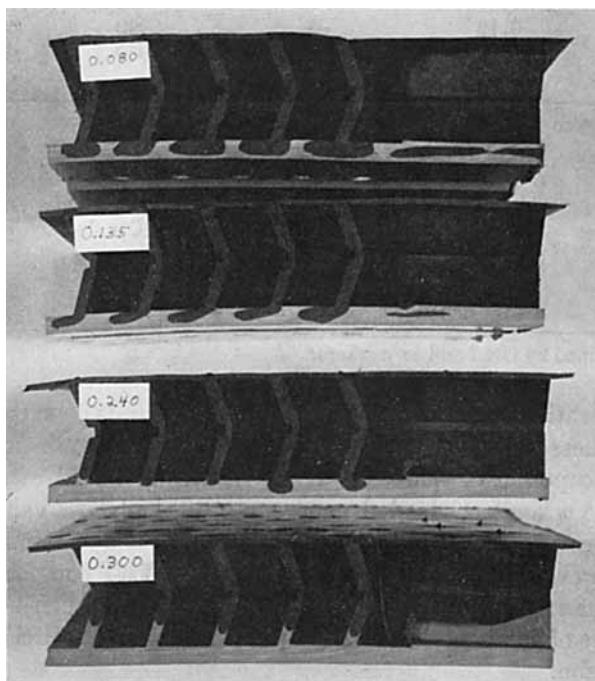


Fig. 20. Flow pattern as a function of inserted rubber pad thickness.

The mold is closed, bumped to vent trapped air, and the rubber is transferred into the mold. The part is then cured at  $300^{\circ}\text{F}$  for 35 min, demolded, and postcured.

Fabrication of full-size development pads (14 in.  $\times$  17 in.  $\times$   $\sim 2.00$  in.) from formulation JM-G, Table I, gave parts that met all desired properties except that, on repeated static cycling to 60% deflection, cracks developed in the strut. Using two color moldings as shown in Figure 20, the strut cracking was traced to a knit line failure due to the rubber flow pattern and the resulting concentration of mold release agents in the knit line. Thickness of the rubber-Teflon composite was found to be critical, as location of the knit line in the strut or in the pad face could be controlled by proper thickness selection.



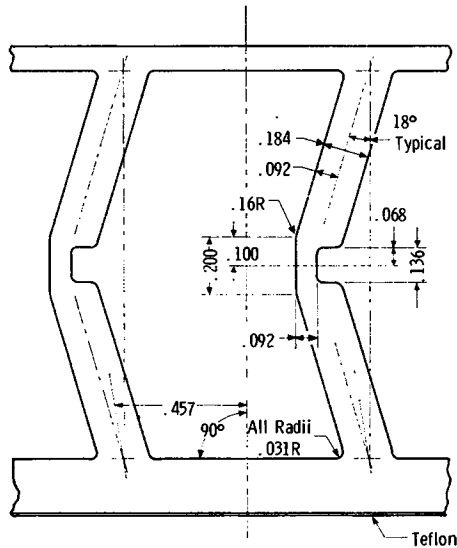


Fig. 21. Strut design HC-11.

By complete removal of external mold release agent (i.e., release agent on core bars), the problem of knit line failure was greatly reduced. Also, by thinning the Teflon-rubber composite to  $\sim 0.075$  in., the knit line was moved to the pad surface where flexing is not as great as in the beam of the strut. With the absence of mold release, however, demolding became almost impossible and a considerable amount of rubber tearing resulted.

Coating the core bars with a baked-on Teflon surface (E. L. Stone Co., 2998 Eastern Road, Barberton, Ohio—coating 851-204) resulted in much easier demolding of the part and reduced the rejection rate due to tearing.

Nearly simultaneously with the knit line failure due to mold release and the Teflon coating of the bars, continued engineering studies indicated the need to use a longer overall strut length without increasing the overall pad thickness of  $\sim 2.00$  in. In order to increase the plateau region of the load-deflection curve, the thickness of the face pads was reduced from 0.250 in. to 0.160 in. and the thickness of the Teflon-rubber preform from 0.160 in. to 0.100 in. The new strut design with longer struts and thinner face sheets was designated HC-11. Figure 21 shows a cross section of the HC-11 strut, and Figure 22 shows the static compression-deflection limits for the HC-11 strut.

The longer strut length increases the flow path distance for the transferred stock requiring a formulation with greater scorch life than the marginal compound G of Table I. Better flex resistance was desired, and some internal mold release agents and factices were evaluated to enhance flow.

With the strut shape (HC-11) and strut thickness (0.185 in.) redefined, the remaining variable of the formulation was approached using compound JM-G, Table I, as a starting point.

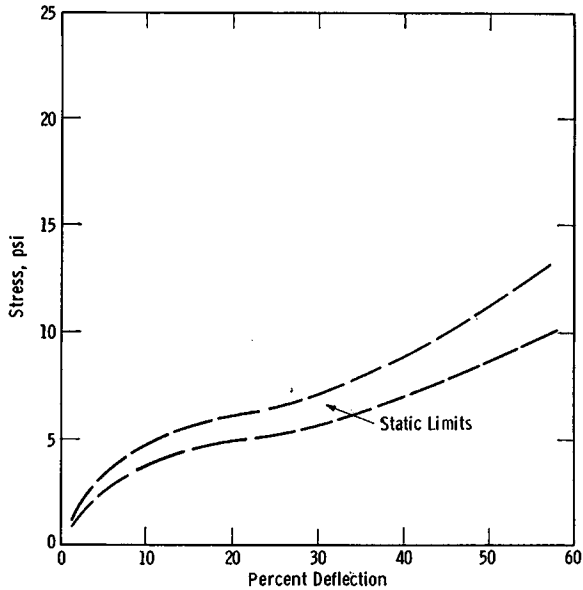


Fig. 22. Static compression-deflection envelope for neoprene pads. HC-11 strut design.

Since demolding and strut cracking were problems on full-scale development-size pieces only, it was necessary to fabricate full-size pads containing various internal mold release agents to solve demolding without affecting other response characteristics. The release agents evaluated are listed in

TABLE III  
Internal Mold Release Agents and Process Aids

	Effectiveness	Comments
Mold Release		
Polyethylene (low MW)	aids demolding, little effect on physical properties	interferes with knitting of transferred stock
Nitrile rubber (Paracril BLJT)	aids demolding	D/S ratio increases unfavorably
Rubberol	promotes flow, mold release, and knitting	most satisfactory of agents studied; low melting soap
Process Aids		
Amberex	promotes mold flow, gives good finish	effective concentrations >4 phr; gives slight cure delay; dry crumb
Adaphax	promotes mold flow, reduces Mooney	Effective concentrations >4 phr; reduces stiffness; dry crumb.
Fortex	good mold flow, part finish and knitting	cure accelerated, good aging; heavy paste

Table III. Actual demolding can be quite a variable activity—the part either demolds relatively easily or with great difficulty. Polyethylene was rejected because prior experience had demonstrated interference with knitting although flow was promoted. Nitrile rubber (Paracril BJLT) was added as a possible aid in demolding. Although demolding was significantly easier with the nitrile rubber present, as little as 4 parts caused the D/S ratio to exceed the acceptable limit of 2.<sup>10</sup> As mentioned previously, higher levels of nitrile (up to 16 parts) caused the D/S ratio to approach 2.6.<sup>10</sup>

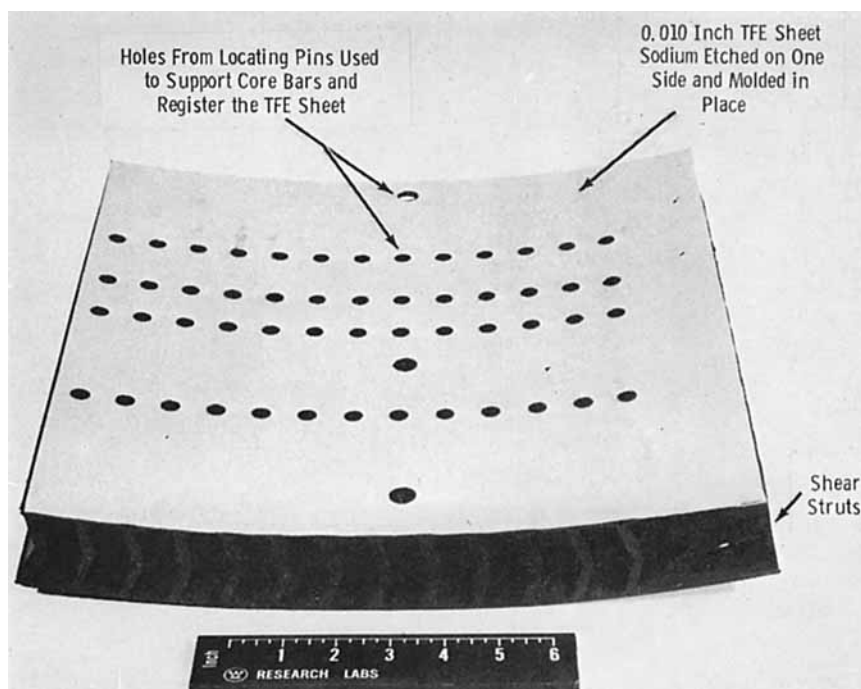


Fig. 23. Full-size neoprene liner pads.

Other agents evaluated were Adaphax (a sulfurless vulcanized vegetable oil), Amberex, Fortex, and Rubberol. Of the various materials tested, it was reported by our fabricator that compounds containing Rubberol gave the best release.

With this information in hand, formulation HM-24, Table I, molded and tested in a small-scale evaluation, proved to be satisfactory from the standpoint of D/S,  $Q$ , static cycling, and the other functional requirements. Development-size pads fabricated at Republic Rubber Company, as shown in Figure 23, were tested for repeated static cycling resistance and were found satisfactory as they exhibited no evidence of crack formation after 500 static cycles to 60% deflection.

TABLE IV  
Physical Property, Molecular Weight Between Crosslinks, and Static Cycling Data  
on Production Pads Containing 128 Parts FT Carbon Black

Sample	Days aged at 70°C	$\bar{M}_c^a$ , g/mole	Tensile properties <sup>b</sup>				Static cycling on postcured pads
			Tensile strength, psi	100% Modulus	Elongation, %		
JM3-122A (control) <sup>c</sup>	0	3190	1328, 1327	—	260, 264	>1000 cycles; no cracks	
JM3-122B (control) <sup>d</sup>	0	2270	1308, 1274, 1490	1362	170, 160, 121	415 cycles; no cracks	
JM3-139A <sup>d</sup>	5	2050	1525	1425	130		
JM3-139B <sup>d</sup>	10	2090	1590	1520	125		
JM3-139C <sup>d</sup>	17	1975	1600	1520	115		
JM3-139D <sup>d</sup>	24	1890	1680	1615	115		
JM3-139E <sup>d</sup>	31	2090	1690	1665	105		

<sup>a</sup> Average of two determinations (by method of ref. 6).

<sup>b</sup> Average of three determinations (ASTM D412).

<sup>c</sup> No postcure.

<sup>d</sup> Postcure of 6.5 hr at 300°F.

The rubber processing, the molding operation, and the molded pads were evaluated from a production point of view. The formulation was deemed processable on an open mill or Banbury, and the pads were moldable and, more importantly, demoldable on a production schedule. With demolding and flex fatigue no longer a problem, compound HM-24, Table I, evolved into compound 808-79, Table I. An early development order was fabricated, sent to the Westinghouse Sunnyvale division, and deemed acceptable. After about 3 months of aging, however, the pads were found to have increased in compression-deflection by  $\sim 5\%$  at 0.8- and 0.9-in. deflections. This increase caused concern regarding the permanence in compression-deflection properties of the neoprene pads. Crosslink density determinations using the technique of Cluff and Gladding<sup>6</sup> clearly demonstrated that the pads exhibiting growth were undercured (Tables II and IV). A postcure study was instigated with simultaneous decrease in carbon black loading from 140 to 116 phr to offset the increase in polymer stiffness. From these specimens it was found that pads with 128 phr carbon black and between 5 and 7 hr of postcure at 300°F gave the desired compression-deflection response and were quite stable on aging or long-time storage.<sup>13</sup>

A complete discussion of long-term storage stability of neoprene liner pads will be the subject of a future paper. However, data in Table IV indicate the significant decrease in molecular weight between crosslinks,  $\bar{M}_c$ , as a function of postcure and postcure followed by aging. The  $\bar{M}_c$  values seem to level off after the 6.5-hr postcure and remain relatively invariant as additional aging is imposed. Physical properties tend to parallel  $\bar{M}_c$  values, as shown by tensile data which are fairly constant after 6.5 hr of postcure at 300°F.

Launch tube liner pads (see Fig. 23 for a photograph of a full-scale pad) are presently being fabricated on a production basis. Periodic full-scale tests indicate that a high level of reproducibility and reliability is inherent in the combination of design and polymer ultimately selected.

## CONCLUSIONS

A missile launcher tube liner has been designed employing a buckling strut concept. Using either urethane<sup>1,2</sup> or neoprene formulations, the compression-deflection and shear characteristics of the basic design can be varied in a predictable manner by changes in strut geometry and polymer system. Full-scale curved liner sections have been produced on a development basis and are currently in production. Liner pads are being installed in the Poseidon missile-carrying submarines at the present time.

The work at the Westinghouse Research and Development Center was done with the guidance and cooperation of the Missile Launching and Handling Department of the Westinghouse Electric Corporation at Sunnyvale, California. The authors are especially grateful to Mr. G. B. Rosenblatt for his interest and active guidance in this project.

### References

1. H. J. Connors, M. A. Mendelsohn, R. H. Runk, and G. B. Rosenblatt, *J. Environ. Sci.*, **27** (June 1968).
2. M. A. Mendelsohn, R. H. Runk, H. J. Connors, and G. B. Rosenblatt, Polyurethane Liner Materials for the Poseidon Launcher, Westinghouse Scientific Paper 68-8B7-HONEY-P1, in press.
3. Private communication from Westinghouse Marine Division, Sunnyvale, California, to Westinghouse R&D Center, Pittsburgh, Pennsylvania.
4. H. F. Minter and J. F. Meier, unpublished results.
5. H. J. Connors and E. S. Diaz, unpublished results.
6. E. F. Cluff, E. K. Gladding, and R. Pariser, *J. Polym. Sci.*, **45**, 341 (1960).
7. H. F. Minter and J. F. Meier, unpublished results.
8. M. A. Mendelsohn, paper presented at Gordon Research Conference on Chemistry and Physics of Cellulose Materials, August 1969.
9. H. F. Minter and J. F. Meier, unpublished results.
10. H. F. Minter and J. F. Meier, unpublished results.
11. H. F. Minter and J. F. Meier, unpublished results.
12. H. F. Minter and J. F. Meier, unpublished results.
13. G. E. Rudd and J. F. Meier, unpublished results.

Received August 6, 1970